A multiscale meshless parametrization for full waveform inversion

Franciane Conceição Peters[1 4], Edivaldo Figueiredo Fontes Junior[2 4], Webe João Mansur[1 4], Djalma Manoel Soares Filho[3], Cid da Silva Garcia Monteiro[1 4], Paulo Frederico Souza Lomeu[1 4], Raphael Vieira Menezes de Souza[1 4], [1]Federal University of Rio de Janeiro/COPPE/PEC, Rio de Janeiro, Brazil. [2]Rural Federal University of Rio de Janeiro, Rio de Janeiro, Brazil. [3]CENPES-PETROBRAS, Rio de Janeiro, Brazil. [4]LAMEMO – Modelling Methods in Engineering and Geophysics Laboratory

This paper was prepared for presentation during the 15th International Congress of the Brazilian Geophysical Society held in Rio de Janeiro, Brazil, 31 July to 3 August, 2017.

Abstract

Full waveform inversion is a technique to recover images of the subsurface using data from a seismic survey. Since it is an ill-posed problem, one of the strategies to regularize the solution is a suitable choice of parameterization. Depending on the parameterization strategy, the solution is searched in a space with certain features that may be convenient to the problem. Furthermore, in general, a parameterization that can represent well the solution with a reduced number of parameters demands less computational effort, and the solution may be robust due to the limited number of degrees of freedom. Here the parameterization is based on a meshless technique that uses Wendland's functions as basis functions to interpolation. Moreover, the spatial distribution of the unknowns is non-uniform, allowing automatically improving the quality of the image near the discontinuities of a velocity model. With some numerical experiments of acoustic inversion of synthetic data, we show that it is possible to represent complex velocity models with a reduced number of parameters if the basis functions are suitable.

Introduction

Full waveform inversion is a technique first stated in 80's (Tarantola, 1984) to recover an image of the subsurface using data from a seismic survey, producing high-quality results. Among many aspects that influence inversion, like noise in data or the description of the physical system (Tarantola and Valette, 1982), a special attention should be given to the choice of parameters. Since regularization means to give preference to models that reflect prior knowledge or expectation, ensuring the convergence towards physically meaningful models (Fichtner, 2011), the choice of a set of parameters could be considered a kind of regularization strategy.

The use of local functions for full waveform inversion is suitable since sharp contrasts in physical properties are expected. Moreover, the standard strategy is to define one parameter for each unknown of the numerical method used to solve the forward problem (Fichtner, 2011). Therefore, the spatial discretization of the forward problem depends on the stability criteria of the numerical method and the suitable representation of the physical properties. On the other hand, the parameterization depends on the resolution and the size of the structures that are expected to be resolvable.

In this work we propose a parameterization methodology that deals with different degrees of freedom for the forward problem and inverse problem. This parameterization is based on a particular set of basis functions called Wendland's functions (Wendland, 1995). These functions can be used to generate 2D and 3D models with specific continuity classes. Each basis function has one basis point and to each one, there is an associated parameter. The set of basis points is distributed uniformly or non-uniformly in the model, as a cloud of points, which allows increasing the resolution in regions of interest. Moreover, in order to be able to represent the physical properties, the region influenced by each basis function must be larger than in the standard block parameterization.

In order to avoid excessive smoothing near discontinuities of the physical model, we suggest a non-uniformly basis points distribution. Such strategy is based on the "spring analogy" (Kazeroni and Afshar, 2015) and tries to concentrate more unknowns near regions of interest.

Numerical experiments demonstrate that the proposed parameterization is able to represent complex models of physical properties and, in the context of multiscale approach, could provide images as good as the images obtained with the standard strategy.

Method

Our main objective is to show that it is possible to generate suitable images using a number as small as possible of parameters which could lead to a reduction of the required memory and the number of operations demanded, an important feature for seismic inversion on 3D imaging and multiparameter inversion. Another feature is to increase the robustness of the inversion methodology because the use of a small number of degrees of freedom can be a regularization strategy. On the other hand, the use of a limited number of parameters requires interpolation to generate velocity models, which can excessively smooth the interfaces between regions with different physical properties.

Another point is related to the discretization required by the numerical method to satisfy its stability criteria. Very often, such discretization is finer than that required by the image resolution.

Using a meshless parameterization, the same parameters can be used to generate models of structured or unstructured meshes for different numerical methods:

Finite Differences (Hustedt et al., 2004), Continuous or Discontinuous Finite Elements (Brossier et al., 2009) and coupled methods (Mansur et al., 2016). Moreover, the methodology is suitable to provide focus in a particular region even when the numerical method employs uniform meshes.

Each parameter is related to a basis point and those are distributed all over the model uniformly or non-uniformly. As mentioned, interpolation tends to smooth the interfaces or discontinuities of the velocity model. However, if we approximate two basis points to the discontinuity, the smoothing is reduced and the image near the interface becomes better than when the points are far from the discontinuity. So, here we propose a methodology to spread the basis points based on an automatic identification of the interfaces concentrating more basis points near the interfaces and reducing the density of basis points over homogeneous areas based on the “spring analogy method.”

In order to analyze the benefits of the non-uniform meshless parameterization, we compare two different strategies, summarized as follows:

• Blocks: The classical constant by parts parameterization, in which a different velocity value is associated to each pixel of the image;

• Meshless: The parameterization is based on interpolation of Wendland’s functions with basis points distributed by the spring analogy, with more points close to the interfaces.

The number of parameters affects the quality of the solution. The interpolation of a reduced number of parameters is more likely to generate smooth models. The excessive smoothing must be avoided because FWI has the potential to recover a high-resolution image, revealing smallest detectable structures.

To minimize the smoothing produced by interpolation, we propose the use of a non-uniform distribution of the basis points clustering them near the discontinuities to avoid excessive smoothing. The non-uniformly distribution concentrates more basis points near the discontinuity or where the gradient of the function varies abruptly.

Since a non-uniform distribution of the basis points gives better approximations than a uniform distribution, the question is: How to compute the ideal position (or a better position) of the points, if the velocity model is not known in the context of seismic inversion? The method we are proposing uses the current velocity model to generate an auxiliary image that represents the possible discontinuities of the model. Then, from a uniform cloud of basis points, the spring analogy is applied to find the new positions, concentrating more points near the discontinuities to reduce smoothing and improving the velocity model.

At the end of the minimization process, when the imaging frequency changes, we use the current image to draw automatically the interfaces. After that, we consider the existence of springs linking each basis point to its neighbors. If a spring crosses an interface, we assume that its stiffness is greater than the stiffness of springs that do not cross interfaces. So, each basis point is subjected to a system of forces, depending on the stiffness and lengths of the springs connected to it. In order to reach the equilibrium of forces, the length of each spring has to change, leading to the new distribution of basis points. In other words, two points linked by a segment that crosses an interface will approximate one to the other. If not, one will depart from the other.

Thus, at the end of the inversion procedure, the model computed with this strategy is supposed to be better than the one computed without the spring analogy, since the former was developed to minimize smoothing near the interfaces.

The use of the spring analogy gives a system of linear equations that represents the equilibrium of forces at all basis points. The size of the system is the number of basis points or unknowns of the inverse problem.

In this work we adopt an adaptive strategy in order to increase the number of parameters as the imaging frequency increases. In this point we apply the spring analogy. Since we are solving the problem with a sequential multiscale approach, we have to be careful when the number of parameters increases. The image obtained with the greater number of parameters must be similar to the old one. In order to do that, after the final distribution of basis points, we have to find the values of parameters that best fit the old image. It is done by solving the normal equations, a linear system with size equal to the number of basis points. As we will see, the proposed methodology behaves well when the adaptive strategy is applied due to the smoothness. The same does not happen with the block parameterization due to the lack of flexibility.

Results

Part A

In order to test if the meshless parameterization is able to fit complex velocity models, we performed 22 numerical experiments. We have used 11 different numbers of parameters and we have compared the images obtained with blocks parameterization and the proposed meshless parameterization. In each experiment, the algorithm looks for the values of parameters that best fit the true velocity model. In all experiments, the true velocity model was created based on a section of the 3D Salt Dome model, Figure 1(a), with 338x160 samples.

Figure 1 shows the true velocity model and the images obtained with both methodologies with four different discretization levels. It is interesting to observe that a small number of parameters gives excessively smooth images if the meshless parameterization is used. It is expected because of the properties of the function we use to interpolate the solution. On the other hand, the blocks parameterization gives images with visible squares, even for the greatest number of parameters we have used. This causes difficulty to fit the interfaces and greater errors than the meshless strategy.

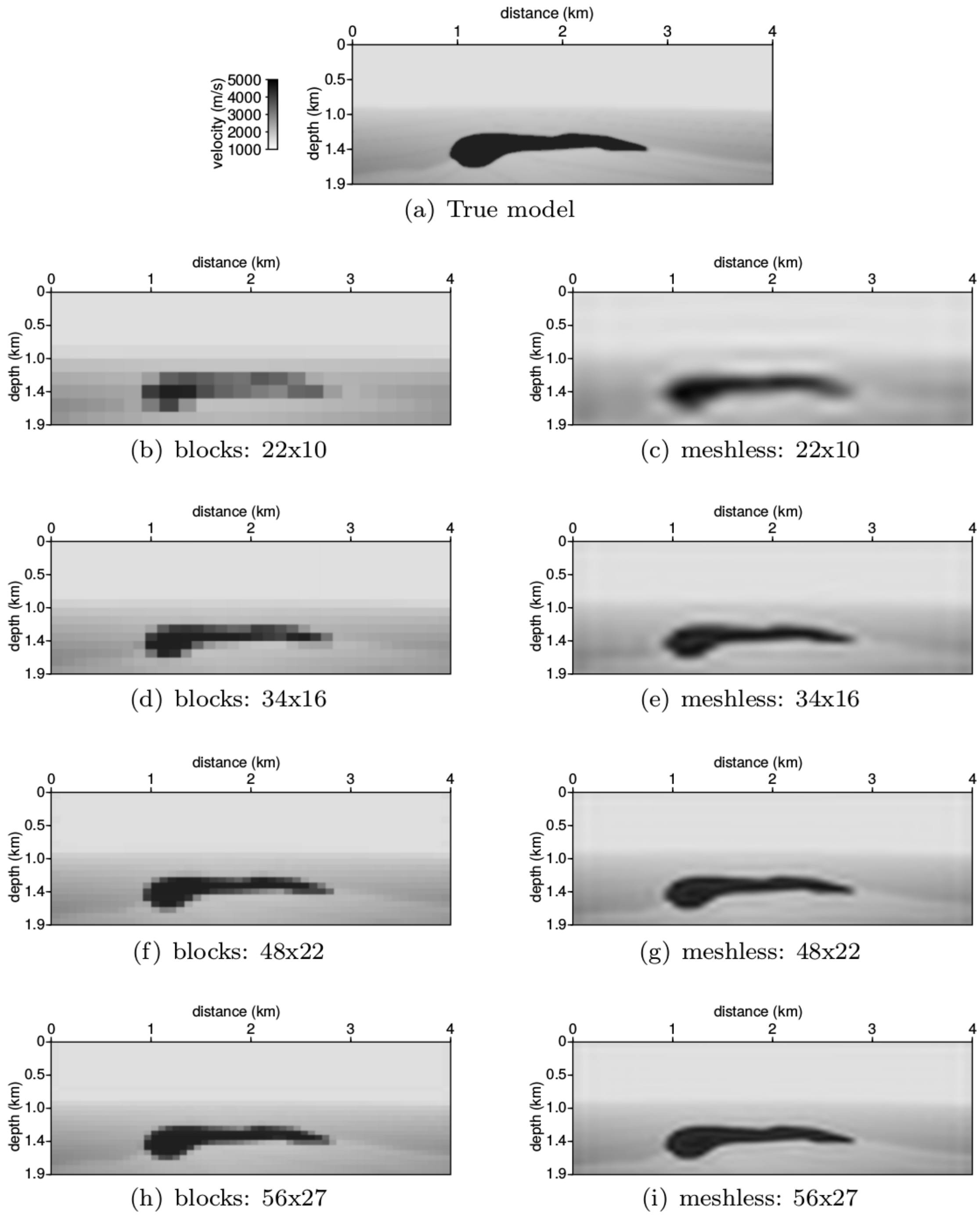

Figure 1 *– The true model (a) and eight images obtained with blocks and meshless parameterization for different discretization levels.*

Each obtained image was compared to the true model, and we have computed the average error and the maximum error. Since, in general, the maximum error occurs along the interface between regions with different velocities, we can consider better the method that gives smaller maximum error. Figure 2 shows the maximum error for each discretization level. In this figure it is possible to see that smaller the number of parameters greater the error, showing the difficulty to fit a complex model using a small number of parameters, as expected. The same figure shows that for each discretization level, the proposed parameterization gives better results than the traditional one, with blocks. The true model could be perfectly fitted with 54.080 parameters (338x160) and we have used less than 3% of this number to test both methodologies.

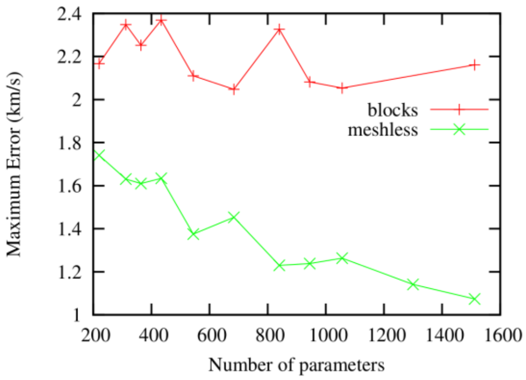

***Figure 2** – The value of maximum errors for each image obtained for 11 discretization levels using two parameterization strategies: blocks and meshless.*

Part B

We have performed three inversion experiments to verify the behavior of the proposed methodology.

First, we have used the true model, the same used in Part A, to generate synthetic seismic data using a finite differences scheme to solve the acoustic wave equation. We have simulated a "split-spread" survey with 82 shots and 168 receivers. The initial model used as input to the inversion algorithm is the true model after smoothing and extraction of the salt dome. The multiscale approach was adopted with the following imaging frequencies: 1.5, 3.0, 4.5, 6.0, 6.9, 7.8, 8.7, 9.6, 10.5, 11.4, 12.3, 13.2, 14.1, 15.0, and 15.9Hz. For each frequency, 20 iterations of the L-BFGS algorithm were performed. The synthetic seismic data were inverted using three strategies:

- With blocks parameterization using the number of parameters that could fit the true model (338x111), here called standard strategy;
- With blocks parameterization starting with 260 (24x11) parameters, increasing the refinement as the frequency increases, and finishing with 6532 (142x46) parameters;
- With the proposed meshless parameterization, starting with 260 and finishing with 6532 parameters.

It is important to emphasize that a layer composed of water with 700 meters is considered known by the inversion algorithm. Figure 3(a) shows the average error between the inverted model and the true model in m/s for each iteration and Figure 3(b) shows the data misfit.

Figure 4 shows the true model, the initial model, and the images obtained by inversion of synthetic seismic data after 300 iterations.

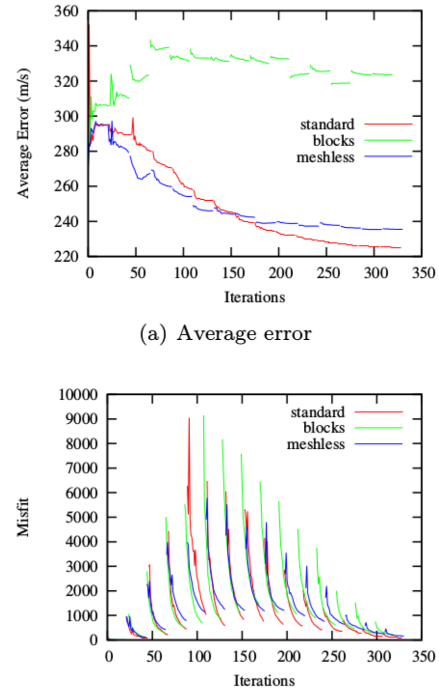

(a) Average error

(b) Misfit

***Figure 3** – The average error of the images obtained with three parameterization strategies (a) and the misfit (b) at each iteration.*

It is possible to see, in Figure 3, that the standard strategy gives the best solution since it has the enough number of parameters to fit the true model. However, the solution is not exact because the number of iterations was limited and the forward model was different from that one used to generate synthetic data. Furthermore, the meshless parameterization was able to fit the initial model as well as the standard parameterization, while the block parameterization was not.

The discontinuities of the curves in Figure 3 represent the change of imaging frequency. Regarding the transition between frequencies, the blocks parameterization was more affected by the refinement strategy. While the model is smooth, up to 150 iterations, the meshless parameterization was better than the standard one. After that, due to the reduced number of parameters, the meshless parameterization was not as good as the standard one. With the reduced number of parameters, the meshless parameterization can be considered superior to the blocks strategy.

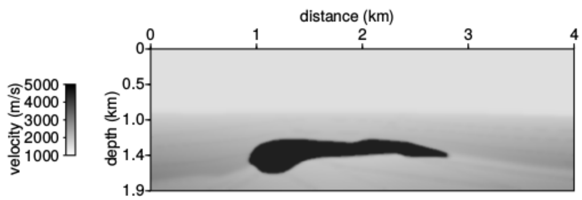

(a) True model

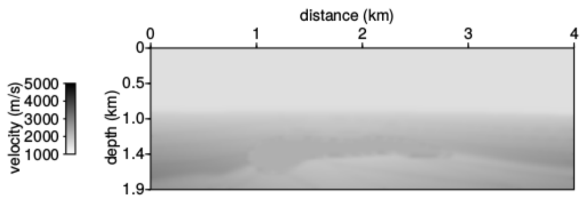

(b) Initial model

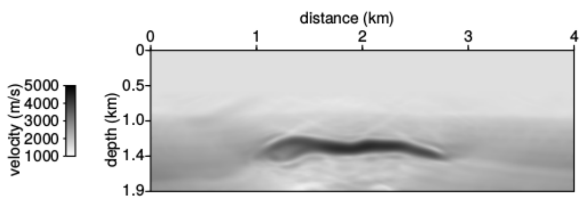

(c) Standard Solution

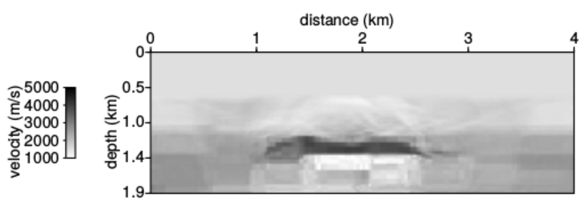

(d) Blocks Solution

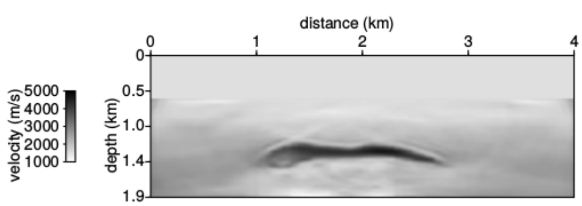

(e) Meshless Solution

***Figure 4** – The true model (a) and the results of inversion with the standard strategy (b), the blocks parameterization (c), and the proposed meshless parameterization(d).*

In Figure 4, it is possible to note that the image obtained with the meshless parameterization is similar to the image obtained with the standard parameterization. The image obtained with blocks parameterization was not able to fit the shape of the top of the salt dome due to the reduced number of parameters and lack of flexibility.

Conclusions

The results show that the proposed meshless parameterization has the potential to represent complex velocity models with a reduced number of parameters. Additionally, the methodology we have presented to distribute the basis points non-uniformly was tested and can be considered suitable, allowing better images by controlling the distribution of basis points near discontinuities.

Depending on the inverse problem, reduced number of parameters leads to a substantial reduction in the computational effort to compute the gradient, compensating the additional computational efforts with the interpolation and the distribution of the basis points. So, the reduced model space presented here is suitable to solve problems in which the computational cost to solve them is proportional to the number of parameters..

Acknowledgments

The authors would like to acknowledge FAPERJ (201.453/2014, 210.210/2016, 210.196/2016), CNPq (306933/2014-4), and Petrobras (ANPETRO-9537, CENPES-13426) for the financial support.

References

Afshar, M., M. Naisipour, and J. Amani, 2011, Node moving adaptive refinement strategy for planar elasticity problems using discrete least squares meshless method: Finite Elements in Analysis and Design, 47, 1315 – 1325.

Aster, R. C., B. Borchers, and C. H. Thurber, 2005, Parameter estimation and inverse problems, 1. ed.: Elsevier Academic Press.

Berenger, J. P., 1994, A perfectly matched layer for the absorption of electromagnetic waves: J. Comput. Phys., 114, no. 2, 185–200.

Blom, F. J., 2000, Considerations on the spring analogy: International Journal for Numerical Methods in Fluids, 32, 647–668.

Bourgeois, A., M. Bourget, P. Lailly, M. Poulet, P. Ricarte, and R. Versteeg, 1991, Marmousi, model and data: Presented at the Proceedings of 1990 EAEG Workshop on Practical Aspects of Seismic Data Inversion.

Brossier, R., S. Operto, and J. Virieux, 2009, Seismic imaging of complex onshore structures by 2d elastic frequency-domain full-waveform inversion: Geophysics, 74, WCC105–118.

Clayton, R., and B. Engquist, 1977, Absorbing boundary conditions for acoustic and elastic wave equations: Bulletin of the seismological society of America, 67, 1529–1540.

Fichtner, A., 2011, Full seismic waveform modelling and inversion: Springer.

Firoozjaee, A., and M. H. Afshar, 2012, Error estimate and adaptive refinement for in compressible navier-stokes equations using the discrete least squares meshless method: International Journal for Numerical Methods in Fluids, 70, 56–70.

Hustedt, B., S. Operto, and J. Virieux, 2004, Mixed-grid and staggered-grid finite-difference methods for frequency-domain acoustic wave modelling: Geophysical Journal International, 157, 1269–1296.

Kaipio, J., and E. Somersalo, 2005, Statistical and computational inverse problems: Springer.

Kazeroni, S. N., and M. Afshar, 2015, An adaptive node regeneration technique for the effcient solution of elasticity problems using {MDLSM} method: Engineering Analysis with Boundary Elements, 50, 198 – 211.

Li, X. S., and J. W. Demmel, 2003, Superlu dist: A scalable distributed-memory sparse direct solver for unsymmetric linear systems: ACM Trans. Mathematical Software, 29, 110–140.

Liu, D. C., and J. Nocedal, 1989, On the limited memory BFGS method for large scale optimization: Mathematical Programming, 45, no. 1, 503–528.

Mansur, W. J., W. L. A. Pereira, C. S. G. Monteiro, R. S. Corrêa, G. T. Santos, C. Dors, F. C. Peters, and E. G. D. do Carmo, 2016, A greens function based procedure to account for non-quiescent past applied to numerical modeling of seismic offshore surveys: Engineering Analysis with Boundary Elements, 55, 67 – 79.

Nakahashi, K., and G. Deiwert, 1987, Self-adaptive grid method with application to airfoil flow: 25.

Nocedal, J., and S. J. Wright, 2006, Numerical optimization: Springer.

Plessix, R. E., 2006, A review of the adjoint-state method for computing the gradient of a functional with geophysical applications: Geophysical Journal International, 167, 495 – 503.

Tarantola, A., 1984, Inversion of seismic reflection data in the acoustic approximation: Geophysics, 49, 1259–1266.

Tarantola, A., and B. Valette, 1982, Inverse problems= quest for information: Journal of geophysics, 50, 150–170.

Wendland, H., 1995, Piecewise polynomial, positive definite and compactly supported radial functions of minimal degree: Advances in Computational Mathematics, 4, 389–396.